Density-functional study of the nematic-isotropic interface of hard spherocylinders

E. Velasco
Departamento de Física Teórica de la Materia Condensada and Instituto Nicolás Cabrera, Universidad Autónoma de Madrid, E-28049 Madrid, Spain

L. Mederos
Instituto de Ciencia de Materiales de Madrid, Consejo Superior de Investigaciones Científicas, E-28049 Madrid, Spain

D. E. Sullivan
Department of Physics and Guelph-Waterloo Physics Institute, University of Guelph, Guelph, Ontario, Canada N1G 2W1
(Received 8 May 2002; published 19 August 2002)

The Somoza-Tarazona density-functional theory is applied to the isotropic-nematic interface of hard spherocylinders with length (L)-to-diameter (D) ratios in the range $L/D=5-20$. Properties such as the density and orientational order-parameter profiles and the variation of interfacial tension with bulk nematic tilt angle agree qualitatively with results of previous studies at larger values of L/D using both computer simulation and the Onsager second-virial approximation. The minimum interfacial tension is obtained at a tilt angle of 90°. For values of $L/D\sim5$, it is found that the Onsager approximation predicts a spurious minimum in the interfacial tension at small tilt angles.

DOI: 10.1103/PhysRevE.66.021708 PACS number(s): 64.70.Md, 61.30.Cz, 61.30.Hn

I. INTRODUCTION

Understanding surface effects in liquid crystals continues to be a topic of both fundamental and technological importance. Recently there has been a resurgence of interest in the interfacial behavior of the most elementary model for liquid crystals, namely, a fluid of rigid hard rods. Using both computer-simulation and density-functional theory, recent works have examined the static properties of the interface between coexisting isotropic and nematic phases [1–5] as well as interfaces of the fluid near a single hard wall or confined between two parallel hard walls [6,7]. The latter two works have also studied associated wetting and capillary condensation effects. So far, the density-functional theories used in these studies have been based on the Onsager second-virial approximation, in some works [6] further simplified by use of Zwanzig's [8] discrete-orientation model. The Onsager approximation becomes exact for the behavior of the isotropic-nematic phase transition when the length-to-diameter (L/D) ratio of the hard rods tends to infinity, since in that limit the coexisting volume fractions tend to zero [9]. However, for finite L/D as well as in the treatment of other possible types of hard-rod phase transitions such as the nematic-smectic-A transition, for which the transition values of the volume fraction are of $O(1)$ even when $L/D\rightarrow\infty$, the Onsager approximation is no longer exact. Extensions of the Onsager approach should then be considered.

In this paper we apply the Somoza-Tarazona (ST) [10] density-functional theory. This theory combines a translation-orientation "decoupling" approximation, originally introduced by Parsons [11] and Lee [12] to extend the Onsager theory to uniform phases of arbitrary density, with an approximate "weighted-density" functional method appropriate for a nonuniform rigid-rod fluid. Recently we described an efficient numerical scheme for solving the ST theory and used it to determine the bulk phase diagram of freely rotating hard spherocylinders [13]. The hard-spherocylinder model is considered here rather than other possible models such as hard ellipsoids, due to the absence of smectic phases in the latter. In the present work, we extend our analysis of the ST theory to the isotropic-nematic interface. As in previous work based on the Onsager approximation, we examine the properties of the density and orientational order-parameter profiles at the interface, including effects of interfacial biaxiality. We also study anchoring behavior indicated by the variation of the interfacial tension as a function of the tilt angle between the nematic director and the interface normal. In agreement with other work, we find that the minimum isotropic-nematic interfacial tension is obtained when the director is parallel to the interface. It is also shown, however, that the Onsager approximation produces spurious minima in the interfacial tension at oblique tilt angles for small elongations $L/D\sim5$, a range not considered in previous work but relevant to many real liquid crystals [14]. For larger L/D, the results of the ST theory and Onsager theory are in good agreement, apart from differences in the predictions of the densities of the coexisting bulk phases.

This work can be considered a preliminary step toward studying a variety of inhomogeneous structures of the hard-spherocylinder fluid, such as interfaces between other types of coexisting phases (e.g., nematic smectic) as well as associated wetting and adsorption phenomena, which will be tackled in future work. In the following section the ST theory is reviewed. Several technical hurdles faced in implementing the theory are discussed in Sec. III. The results are presented in Sec. IV, while a summary and conclusions are contained in Sec. V.

II. MODEL FOR A PLANAR NEMATIC-ISOTROPIC INTERFACE

The molecular model consists of hard spherocylinders of cylinder length L and diameter D. The Helmholtz free-energy

 ©2002 The American Physical Society

functional of a fluid of such molecules is expressed by the sum of the ideal-gas term F_{ID} and an excess term F_{ex} due to interactions. In the Somoza-Tarazona approximation [10], the latter is given by

$$F_{\mathrm{ex}}[\rho]=\int d\mathbf{r}\int d\hat{\mathbf{\Omega}}\rho(\mathbf{r},\hat{\mathbf{\Omega}})\frac{\Psi_{\mathrm{ex}}^{\mathrm{ref}}[\overline{\rho}(\mathbf{r})]}{\overline{\rho}_{\mathrm{ref}}(\mathbf{r})}\int d\mathbf{r}' \times\int d\hat{\mathbf{\Omega}}'\rho(\mathbf{r}',\hat{\mathbf{\Omega}}')V_{\mathrm{exc}}(\mathbf{r}'-\mathbf{r},\hat{\mathbf{\Omega}},\hat{\mathbf{\Omega}}'), \quad (1)$$

where $\rho(\mathbf{r},\hat{\mathbf{\Omega}})$ is the one-molecule distribution function, $\Psi_{\mathrm{ex}}^{\mathrm{ref}}(\overline{\rho})$ is the excess free-energy per molecule of a uniform reference system of parallel hard bodies, and $V_{\mathrm{exc}}(\mathbf{r}'-\mathbf{r},\hat{\mathbf{\Omega}},\hat{\mathbf{\Omega}}')$ is the excluded volume function (i.e., minus the Mayer function) of two spherocylinders with centers of mass at $\mathbf{r}$ and $\mathbf{r}'$ and orientations $\hat{\mathbf{\Omega}}$ and $\hat{\mathbf{\Omega}}'$. We use the standard factorization $\rho(\mathbf{r},\hat{\mathbf{\Omega}})=\rho(\mathbf{r})f(\mathbf{r},\hat{\mathbf{\Omega}})$, where $f(\mathbf{r},\hat{\mathbf{\Omega}})$ is the normalized orientational distribution function. Here the reference system is taken to be a fluid of parallel hard ellipsoids of major and minor diameter $\sigma_{\parallel}$ and $\sigma_{\perp}$, respectively, with molecular volume and aspect ratio $\sigma_{\perp}/\sigma_{\parallel}$ equal to those of the spherocylinders: these conditions uniquely determine the size and shape of the reference ellipsoids. In this case, prescriptions for calculating the two "weighted densities" $\overline{\rho}(\mathbf{r})$ and $\overline{\rho}_{\mathrm{ref}}(\mathbf{r})$ (the latter being proportional to the lowest-order component of the former) in terms of the actual number density $\rho(\mathbf{r})$ are given in Ref. [13]. In a planar geometry, $\rho(\mathbf{r},\hat{\mathbf{\Omega}})=\rho(z,\hat{\mathbf{\Omega}})$ depends only on the spatial coordinate z normal to the interface, so that the interfacial tension functional γ (i.e., excess grand potential per area over that of the coexisting bulk fluids) reads

$$\beta\gamma[\rho]=\int_{-\infty}^{\infty}dz\left\{\rho(z)\left[\log\rho(z)-1-S_{\mathrm{rot}}(z)-\beta\mu+\frac{\beta\Psi_{\mathrm{ex}}^{\mathrm{ref}}[\overline{\rho}(z)]}{\overline{\rho}_{\mathrm{ref}}(z)}\int_{-\infty}^{\infty}dz'\rho(z')V_{\mathrm{eff}}(z,z';[f])\right]+\beta p\right\}, \quad (2)$$

where $\beta=(kT)^{-1}$. Here S_{rot} is the local rotational entropy, defined in Eq. (26) in Ref. [13], μ the bulk chemical potential, and p the bulk pressure. The function V_{eff} is a double angular average, weighted by the function f, of the excluded area between two spherocylinders at heights z and z' (see following section).

In the limit of vanishing number density, the ratio $\beta\Psi_{\mathrm{ex}}^{\mathrm{ref}}(\overline{\rho})/\overline{\rho}_{\mathrm{ref}}\rightarrow 1/2$ [15]. In this limit, the functionals in Eqs. (1) and (2) become equivalent to those of the Onsager second-virial approximation [1–3,5,6]. Therefore, on replacing that density-dependent prefactor by 1/2, the numerical calculations of the present theory can be trivially modified to reproduce results of the Onsager theory.

As in Ref. [13], here we parametrize the orientational distribution function as

$$f(z,\hat{\Omega})=\frac{\exp[\Lambda_1(z)P_2(\cos\theta)+\Lambda_2(z)\sin 2\theta\cos\phi+\Lambda_3(z)\sin^2\theta\cos 2\phi]}{\int d\hat{\mathbf{\Omega}}\exp[\Lambda_1(z)P_2(\cos\theta)+\Lambda_2(z)\sin 2\theta\cos\phi+\Lambda_3(z)\sin^2\theta\cos 2\phi]}, \quad (3)$$

where θ and ϕ are the polar and azimuthal angles of a molecule with respect to the space-fixed Cartesian axes, and $P_2(x)$ is the second-order Legendre polynomial. Due to the dependence on the angle ϕ, this parametrization allows for the possibility of biaxial interfacial states [16,17], and is equivalent to an expansion of $\ln f(z,\hat{\Omega})$ up to second-rank spherical harmonics [1,2]. The parametric functions $\Lambda_i(z)$ can be considered as effective one-body external potentials. Consistent with the last equation, the orientational order of the fluid is described by the following three order parameters, which are the projections of $f(z,\hat{\Omega})$ in the second-rank spherical harmonic subspace and which are uniquely related to the functions $\Lambda_i(z)$:

$$\eta(z)=\int d\hat{\mathbf{\Omega}}P_2(\cos\theta)f(z,\hat{\mathbf{\Omega}}), \quad (4)$$

$$\sigma(z)=\int d\hat{\mathbf{\Omega}}\sin^2\theta\cos 2\phi f(z,\hat{\mathbf{\Omega}}),$$

$$\nu(z)=\int d\hat{\mathbf{\Omega}}\sin 2\theta\cos\phi f(z,\hat{\mathbf{\Omega}}).$$

As in Ref. [13], one could adopt these order parameters together with the number density $\rho(z)$ as the variational functions of the theory. However, it proves more convenient from a computational point of view to use a different set of orientational order parameters $\eta_p(z),\sigma_p(z)$, referred to a local principal-axis reference frame defined by the local nematic director. The two reference frames are connected through a rotation from the z axis by an angle $\psi(z)$, the local *tilt angle*. The relation between both sets of order parameters, $\{\eta(z),\sigma(z),\nu(z)\}$ and $\{\eta_p(z),\sigma_p(z),\psi(z)\}$ is [18]

$$\eta(z)=\eta_p(z)P_2[\cos\psi(z)]+\frac{3}{4}\sigma_p(z)\sin^2\psi(z), \quad (5)$$

$$\sigma(z)=\eta_p(z)\sin^2\psi(z)+\frac{1}{2}\sigma_p(z)[1+\cos^2\psi(z)],$$

$$\nu(z)=\left[\eta_p(z)-\frac{1}{2}\sigma_p(z)\right]\sin 2\psi(z).$$

Use of the principal-axis order parameters simplifies the calculation of the orientational entropy [13], since the latter is rotationally invariant and, therefore, does not depend on the tilt angle $\psi(z)$. As indicated in the following section, the principal-axis order parameters are also more convenient in accounting for the boundary conditions on the orientational order in the bulk nematic phase. This approach requires inverting Eqs. (4) to determine the functions $\Lambda_i(z)$ in terms of $\eta(z)$, $\sigma(z)$, and $\nu(z)$, and, in turn, in terms of the principal-axis order parameters $\eta_p(z)$, $\sigma_p(z)$ and $\psi(z)$ using the transformation formulas (5). This inversion is done beforehand and the results stored in a large table. An alternative and equivalent approach would be to use the Λ_i's as independent variables, and perform the free-energy minimization with respect to these variables.

III. SOME TECHNICAL CONSIDERATIONS

A. Evaluation of the effective potential V_{eff}

The function V_{eff} is given by

$$V_{\mathrm{eff}}(z,z';[f])=\int d\hat{\mathbf{\Omega}}\int d\hat{\mathbf{\Omega}}'f(z,\hat{\mathbf{\Omega}})f(z',\hat{\mathbf{\Omega}}')\times\int d\mathbf{R}'V_{\mathrm{exc}}(\mathbf{r}'-\mathbf{r},\hat{\mathbf{\Omega}},\hat{\mathbf{\Omega}}'),\tag{6}$$

where $\mathbf{R}'=(x'-x,y'-y)$ is the displacement vector normal to the z axis and translational symmetry with respect to this vector has been invoked. Insofar as the approximate representation for $f(z,\hat{\mathbf{\Omega}})$ in Eq. (3) is employed, and in view of Eqs. (4), we can express $V_{\mathrm{eff}}(z,z';[f])=V_{\mathrm{eff}}(z'-z;\eta(z),\sigma(z),\nu(z);\eta(z'),\sigma(z'),\nu(z'))$, where the orientational order at heights z and z' is indicated by the corresponding order parameters. Note that the solid angles in Eq. (6) are necessarily referred to the space fixed rather than director reference frame. Since we do not know how to calculate V_{eff} analytically and the tabulation of this function appears to be out of the question, the following approximation was used in previous work [13]:

$$V_{\mathrm{eff}}(z'-z;\eta(z),\sigma(z),\nu(z);\eta(z'),\sigma(z'),\nu(z'))\approx V_{\mathrm{eff}}\left(z'z;\frac{\eta(z)+\eta(z')}{2},\frac{\sigma(z)+\sigma(z')}{2},\frac{\nu(z)+\nu(z')}{2};\frac{\eta(z)+\eta(z')}{2},\frac{\sigma(z)+\sigma(z')}{2},\frac{\nu(z)+\nu(z')}{2}\right).\tag{7}$$

Subject to the truncated representation in Eq. (3), this approximation is exact in the bulk nematic phase and very good in the bulk smectic phase, where the spatial variation of the orientational order parameters is very weak. Also, it allows for a dramatic simplication of the calculations since the values of the effective potential can be tabulated, for each value of $z'-z$, as a three-entry table. This strategy has proved to be rather fruitful in our previous works [13,19]. Our original hope was that the same approximation would also be adequate in the case of the smoothly varying nematic-isotropic interface. However, it turns out that the approximation generates an instability that creates density oscillations at the interface, which was not expected *a priori*.

The alternative approach considered here is to evaluate the effective potential exactly [subject to the representation Eq. (3)], with no intervening approximation. Specifically, we calculate the integral

$$V_{\mathrm{eff}}(z'-z;[f])=\int_0^{\pi}d\theta\sin\theta\int_0^{2\pi}d\phi\int_0^{\pi}d\theta'\sin\theta'\int_0^{2\pi}d\phi'\times f(z,\theta,\phi)f(z',\theta',\phi')\times\int d\mathbf{R}'V_{\mathrm{exc}}(\mathbf{r}'-\mathbf{r},\theta,\phi,\theta',\phi').\tag{8}$$

Introducing the notation

$$V_{\mathrm{exc}}(z'-z,\theta,\phi,\theta',\phi')=\int d\mathbf{R}'V_{\mathrm{exc}}(\mathbf{r}'-\mathbf{r},\theta,\phi,\theta',\phi'),\tag{9}$$

and using the symmetry properties of the excluded volume, the integral for V_{eff} can be written as

$$\begin{aligned}V_{\mathrm{eff}}(z'-z;[f])=&\int_0^{\pi/2}d\theta\sin\theta\int_0^{2\pi}d\phi\int_0^{\pi/2}d\theta'\sin\theta'\\&\times\int_0^{2\pi}d\phi'\{[f(z,\theta,\phi)f(z',\theta',\phi')+f(z,\pi-\theta,\phi)f(z',\pi-\theta',\phi')]V_{\mathrm{exc}}(z'-z,\theta,\phi,\theta',\phi')\\&\times[f(z,\theta,\phi)f(z',\pi-\theta',\phi')+f(z,\pi-\theta,\phi)f(z',\theta',\phi')]V_{\mathrm{exc}}(z'-z,\theta,\phi,\pi-\theta',\phi')\}.\end{aligned}\tag{10}$$

The kernels

$$V_{\mathrm{exc}}(z'-z,\theta,\phi,\theta',\phi'), \quad V_{\mathrm{exc}}(z'-z,\theta,\phi,\pi-\theta',\phi')$$

are computed and tabulated prior to the minimization of the functional. As in previous work [13], the z dependence of these kernels is handled via the Fourier expansions

$$V_{\mathrm{exc}}(z,\theta,\phi,\theta',\phi')=\sum_{n=-\infty}^{\infty} V_n^{(1)}(\theta,\phi,\theta',\phi')e^{ik_n z},$$

$$V_{\mathrm{exc}}(z,\theta,\phi,\pi-\theta',\phi')=\sum_{n=-\infty}^{\infty} V_n^{(2)}(\theta,\phi,\pi-\theta',\phi')e^{ik_n z}, \tag{11}$$

with $k_n=n\pi/(L+D)$, so that the quantities that are actually tabulated are the Fourier components $V_n(\theta,\phi,\theta',\phi')$ and $V_n(\theta,\phi,\pi-\theta',\phi')$. Note that in the above expansions the coefficients have the property $V_{-n}^{(i)}=V_n^{(i)}$, so that the resulting expansions are real and involve sums of cosine functions. In practice the expansions are truncated beyond $n>N$ for some value of N.

Calculations using the present procedure are more time consuming than in Ref. [13] but remain within reasonable limits. All numerical integrations, including those for obtaining the Fourier components, are performed using Gaussian quadrature, usually involving 12 roots for each variable of integration, though selected calculations have been done using 20 roots. The number of Fourier components used was $N=15$, with selected checks made using $N=21$.

B. Minimization of the functional

Minimization of the interfacial-tension functional Eq. (2) is performed as usual by first discretizing the z axis so that $\beta\gamma$ becomes a function of a large number of variables, namely, the values of all the order parameters at the mesh points: $\rho_i,\eta_{p,i},\sigma_{p,i},\psi_i$. Typically, the number of mesh points used is 300 and the corresponding spatial step length is $\Delta z/L=0.05$. The ensuing multidimensional minimization is performed using a conjugate-gradient method.

One of the desired results of this study is the value of the equilibrium tilt angle ψ_b in the bulk nematic phase, i.e., the angle between the bulk nematic director and the z axis normal to the interface. We take the bulk nematic phase to be approached as $z\to\infty$ (in practice, outside of a finite "numerical box"). In this limit, the principal-axis order-parameters approach

$$\eta_p(z\to\infty)=\eta_b,$$
$$\sigma_p(z\to\infty)=0, \tag{12}$$
$$\psi(z\to\infty)=\psi_b,$$

where η_b is the bulk nematic order parameter measuring mean molecular orientations relative to the director axis. One expects that ψ_b is actually determined by the interactions near the interface, but its value is not known *a priori*. In particular, we do not know *a priori* how the molecular axes will on average orient near the interface. Therefore, the bulk tilt angle ψ_b should be included as a variable in the minimization process, a procedure which we call *full minimization*, but which is technically nontrivial to carry out due to the fact that ψ_b enters as a boundary condition and hence is of a different nature from the other variational parameters. In practice, we can proceed by *fixing* ψ_b, performing a minimization over the local variables $\rho(z),\eta_p(z),\sigma_p(z)$, and $\psi(z)$, and then scanning over different values of ψ_b so as to locate that value which yields the minimum interfacial tension γ, corresponding to the equilibrium structure at the interface. A similar method has been used in previous studies using density-functional theory for various "Maier-Saupe-type" liquid-crystal models [20,21], and will be called the *partial minimization* method. Complications of this approach arise due to the fact that, although the bulk tilt angle is fixed at each minimization step, all the local order parameters in the model are allowed to vary inside the numerical box. In particular, the local tilt angle $\psi(z)$ may fluctuate and its profile may be nonmonotonic, exhibiting so-called "subsurface deformation" (as found, e.g., in Ref. [21]). We have indeed observed such an effect here, namely, that when the bulk tilt angle ψ_b is fixed at values different from 90°, the local tilt angle does not remain uniform and instead varies with z in order to satisfy the energetically favorable orientation at the interface (which tends to be 90°), even at the cost of seriously distorting the tilt-angle profile in the box between the interface and the bulk nematic phase. In fact, for bulk tilt angles ψ_b near 0°, this frustration effect appears to prevent us from obtaining convergent numerical solutions by the partial minimization method.

In practice, we have proceeded by two slightly different methods based on fixing the bulk tilt angle at each minimization step and assuming that ψ_b is a "slow variable," i.e., would change slowly compared with the local order parameters during a *full minimization* process [20]. In the first approach, called the *first constraint minimization*, we let the conjugate-gradient minimization run for a few iterations only, typically 10, and thereby obtain a *constraint* plot of interfacial tension versus bulk tilt angle, from which the equilibrium configuration is deduced. The second approach, called the *second constraint minimization*, differs from the first in that the local tilt angle is not allowed to fluctuate, so that the tilt-angle profile $\psi(z)$ is constrained to be constant across the box and equal to the bulk value ψ_b. Again, a plot of interfacial tension versus ψ_b allows us to deduce the equilibrium configuration of the interface. These two methods are not rigorous. However, since we are reasonably confident that distorted tilt-angle profiles do not occur at equilibrium in the present model, we have mainly adopted the *second constraint minimization* method and have occasionally implemented the first method as a check.

IV. RESULTS

The theory outlined above is now applied to the nematic-isotropic interface of hard spherocylinders. In fact, the actual results presented below are obtained using a simplification whereby the weighted density $\overline{\rho}(z)$ is replaced by the true

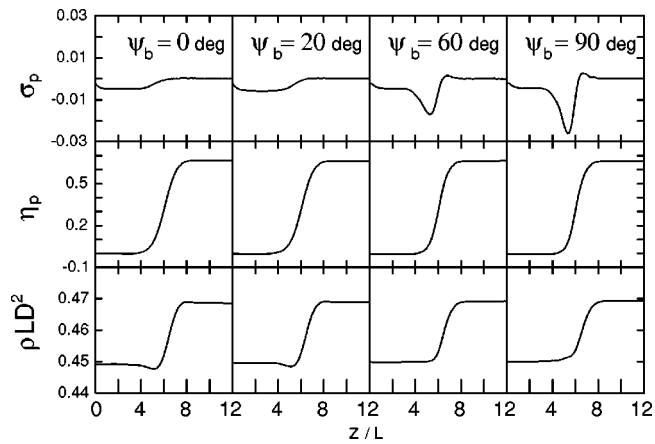

FIG. 1. Density and order-parameter profiles obtained from the extended Onsager theory with the second constraint method, for the case $L/D=5$ and for different bulk tilt angles (indicated on the graphs).

local density $\rho(z)$. This is called the "extended Onsager theory," and is equivalent to a direct extension of the Parsons-Lee [11,12] theory for bulk nematics. This replacement is justified by the expected smoothness of the nematic-isotropic interface and considerably simplifies the numerical analysis: preliminary studies using the full theory indicate that its results differ negligibly from those of the extended Onsager theory.

Figure 1 plots the density and orientational order-parameter profiles for spherocylinders of length-to-diameter ratio $L/D=5$, as obtained from the extended Onsager theory using the second constraint minimization method, for values of the bulk tilt angle $\psi_b=0°,20°,60°$, and 90°. Figure 1 shows that $\eta_p(z)$ is always monotonic, whereas the density $\rho(z)$ is nonmonotonic for small tilt angles (i.e., for bulk director orientations nearly perpendicular to the interface), exhibiting a minimum on the isotropic side of the interface. This represents a slight molecular depletion, an effect which disappears as $\psi_b \to 90°$, i.e., as the bulk director approaches a planar orientation. This feature of the density was found earlier by Chen and Noolandi [22] using the Onsager theory for spherocylinders with $L/D \to \infty$, and more recently by van Roij *et al.* [6] using the Onsager theory for a discrete-orientation model, as well as by McDonald *et al.* [3] in studies by Onsager theory and computer simulations of hard and soft ellipsoids. Figure 1 also shows that the location of the density interface, as inferred, say, from the position of the inflection point in $\rho(z)$, is shifted toward the bulk nematic phase with respect to the location of the interface indicated by the profile of $\eta_p(z)$. This is also in agreement with previous findings [1–3].

The biaxial order parameter $\sigma_p(z)$ in Fig. 1 is also nonmonotonic, exhibiting a pronounced minimum on the isotropic side of the interface whose amplitude increases (as is expected) with increasing tilt angle ψ_b. Again, these features are in qualitative agreement with previous studies by both theory and simulation [2,5,6,23]. The fact that $\sigma_p(z)$ in Fig. 1 is not exactly zero when $\psi_b=0$ is an artifact due to imprecision in the angular integrations involved in calculating the effective potential.

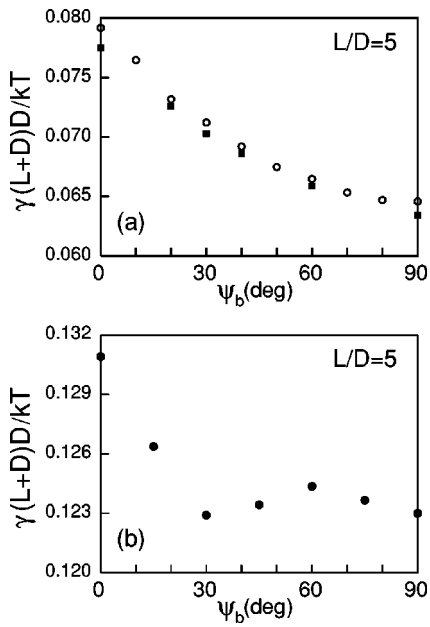

FIG. 2. Interfacial tension vs tilt angle for the case $L/D=5$: (a) results obtained from the extended Onsager approximation using partial minimization with the first constraint method, including only ten iterations (open circles) and from the second constraint method (filled squares); (b) Onsager theory.

Figure 2 shows the behavior of the interfacial tension for $L/D=5$ as a function of the bulk tilt angle ψ_b, as obtained (a) from the extended Onsager approximation using the two minimization techniques and (b) from the Onsager approximation with the second constraint method. The data from the two minimization techniques for the extended Onsager theory are numerically similar. This supports the idea behind the first minimization method, where the conjugate-gradient process is carried out for only ten iterations, namely, that the bulk tilt angle is indeed a slow variable and the *fast* variables, i.e., density and principal-axis order parameters, rapidly accommodate to quasiequilibrium values. Both methods agree that the equilibrium director orientation is parallel to the interface. In the case $\psi_b=90°$, calculations using the second constraint minimization method are equivalent to a full minimization of the free-energy functional with respect to all local variables, since in this case the local tilt-angle profile $\psi(z)$ is found to be constant. The Onsager theory also predicts a minimum in the interfacial tension for a planar director orientation. However, it is seen that the latter theory also exhibits a second minimum with slightly greater depth around a tilt angle $\sim 30°$. We have checked that this finding is not a consequence of numerical inaccuracies, by performing calculations on the Onsager theory using Gaussian quadratures with 20 roots instead of the 12 roots used in other calculations. These more accurate results are shifted downward by an essentially constant amount ($\approx 1\%$) from those obtained with 12 roots, indicating that the numerical inaccuracies are nearly independent of tilt angle. Hence we conclude that the minimum near 30° is a real feature of the

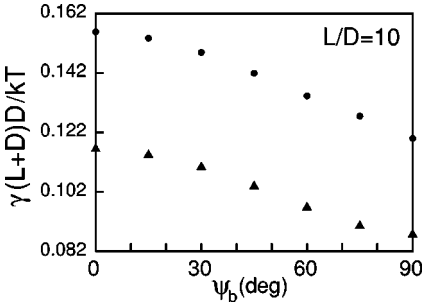

FIG. 3. Interfacial tension vs tilt angle for the case $L/D=10$. Solid circles and triangles indicate results of the Onsager and extended Onsager approximations, respectively.

Onsager theory. This is consistent with the fact that the Onsager theory is not expected to be accurate for such small elongations, and also the fact that such a feature has not been observed in any earlier studies, which have focused on much larger elongations (the minimum aspect ratio considered in computer simulations of ellipsoids by Allen and co-workers is 15 [1–4]). For this reason, we have also applied both the Onsager and extended Onsager theories to the cases $L/D=10$ and 20.

Figure 3 plots the interfacial tension of both theories as a function of ψ_b (second constraint method) for $L/D=10$. In this case, apart from an overall difference in magnitudes, the two theories yield similar behavior of γ, exhibiting a single minimum at $\psi_b=90°$. The values of the interfacial tension at $\psi_b=90°$ according to the two theories, for the three elongations considered here, are listed in Table I along with the reduced number densities of the coexisting isotropic and nematic phases, denoted ρ_{iso} and ρ_{nem}, respectively. These densities are also compared with Monte Carlo values [24]. It is seen that the densities predicted by the extended Onsager theory agree with the Monte Carlo results to within 2.5% in the isotropic phase and to within 4.7% in the nematic phase.

TABLE I. Comparison of theoretical predictions for the bulk densities ρ_{iso} and ρ_{nem} of the coexisting isotropic and nematic phases, and for the reduced interfacial tension γ^* (at bulk tilt angle 90°), for the three elongations considered in this work. The Onsager and extended Onsager approximations are denoted "Ons" and "Ext," respectively, while "MC" refers to Monte Carlo data [24] for the coexisting bulk densities. Values of the latter densities indicated by * are estimates obtained from figures in Ref. [24].

L/D	Theory	$\rho_{\rm iso}LD^2$	$\rho_{\rm nem}LD^2$	γ^*
	Ons	0.8753	0.9442	0.1230
5	Ext	0.4491	0.4686	0.0634
	MC	0.447	0.447	
	Ons	0.4340	0.4821	0.1200
10	Ext	0.2992	0.3290	0.0877
	MC	0.292*	0.320*	
	Ons	0.2145	0.2516	0.1350
20	Ext	0.1759	0.2017	0.1139
	MC	0.172	0.211	

As in the figures, the interfacial tensions in Table I are expressed in the reduced unit $\gamma^*\equiv\beta\gamma(L+D)D$, in order to compare with previous calculations based on the Onsager theory in the limit $L/D\rightarrow\infty$. The most recent analysis gives $\gamma^*=0.156\pm0.001$ for $L/D\rightarrow\infty$ [5]. As seen in Table I, our value for γ^* according to the Onsager theory for $L/D=20$ is still somewhat below this asymptotic limit. Of more significance, the extended Onsager theory yields systematically lower values of γ than the Onsager theory, although the gap decreases with increasing L/D. This is consistent with evidence that Monte Carlo simulations produce slightly lower values of γ than the Onsager theory in the case of hard ellipsoids with length/width ratio of 15 [3]. From Table I, for each value of L/D, the relative difference between the Onsager and extended Onsager values of γ is roughly equal to the relative difference between the corresponding values of the mean density $(\rho_{iso}+\rho_{nem})/2$.

V. CONCLUSIONS

We have examined the structure and free energy of the nematic-isotropic interface of a hard-spherocylinder fluid at molecular length/diameter ratios between $L/D=5$ and 20. The study employs a simplified version of the Somoza-Tarazona [10] density-functional theory, which approximately extends Onsager's classical second-virial theory to arbitrary elongation and density. Qualitatively, most of our results are in agreement with those obtained in earlier studies applying either Onsager theory or computer simulations to hard-rod models with significantly greater elongation [1–3,5–7,22,23]. In particular, the profile of the biaxial orientational order parameter $\sigma_p(z)$, the *weak* nonmonotonicity exhibited by the density profile $\rho(z)$ for small tilt angles ψ_b, and the minimum in the interfacial tension at $\psi_b=90°$, are all consistent with previous studies. We have also shown that the Onsager theory predicts spurious minima in the interfacial tension at small tilt angles for elongations $L/D\sim5$. *A priori*, however, one should not expect the latter theory to be valid in this range of elongations. Our calculations indicate that the present theory yields smaller values of the interfacial tension than the Onsager theory for any finite ratio L/D.

An aspect dwelt upon in this paper is the theoretical determination of the "anchoring angle," i.e., the value of the equilibrium tilt angle ψ_b in the bulk nematic phase. We have discussed several numerical approaches for finding this angle, all of which concur that $\psi_b=90°$, corresponding to planar alignment of the bulk nematic director. We should emphasize, however, that the methods described here are consistent with the finding that the *equilibrium* director structure of the spherocylinder model is characterized by a constant tilt-angle profile $\psi(z)=\psi_b$. For other possible models [20,21,25], our methods do not rule out the occurrence of equilibrium structures exhibiting local deformations of the director while respecting the boundary conditions in the bulk nematic phase.

To our knowledge, no computer-simulation studies of the nematic-isotropic interface of hard spherocylinders in the

range of elongations considered here are available for comparison. Such studies are now being performed by our group and will be described in future work. Recent experiments have measured the interfacial tension of aqueous suspensions of cellulose crystallites characterized by *effective* length/diameter ratios comparable to those considered here [14]. However, as the analysis in Ref. [14] indicates, comparison of the experimental results with ''hard-rod'' models remains problematic due to unresolved effects of electrostatic interactions and polydispersity in particle dimensions.

ACKNOWLEDGEMENTS

This work was supported by Grant Nos. BFM2001-0224-C02-01 and BFM2001-0224-C02-02 from the Ministry of Science and Technology (Spain), and the Natural Sciences and Engineering Research Council (Canada).

[1] M.P. Allen, J. Chem. Phys. **112**, 5447 (2000).
[2] M.S. Al-Barwani and M.P. Allen, Phys. Rev. E **62**, 6706 (2000).
[3] A.J. McDonald, M.P. Allen, and F. Schmid, Phys. Rev. E **63**, 010701 (2001).
[4] N. Akino, F. Schmid, and M.P. Allen, Phys. Rev. E **63**, 041706 (2001).
[5] K. Shundyak and R. van Roij, J. Phys.: Condens. Matter **13**, 4789 (2001).
[6] R. van Roij, M. Dijkstra, and R. Evans, Europhys. Lett. **49**, 350 (2000); J. Chem. Phys. **113**, 7689 (2000).
[7] M. Dijkstra, R. van Roij, and R. Evans, Phys. Rev. E **63**, 051703 (2001).
[8] R. Zwanzig, J. Chem. Phys. **39**, 1714 (1963).
[9] A. Poniewierski, Phys. Rev. A **45**, 5605 (1992).
[10] A.M. Somoza and P. Tarazona, J. Chem. Phys. **91**, 517 (1989); Phys. Rev. A **41**, 965 (1990).
[11] J.D. Parsons, Phys. Rev. A **19**, 1225 (1979).
[12] S.-D. Lee, J. Chem. Phys. **87**, 4972 (1987).
[13] E. Velasco, L. Mederos, and D.E. Sullivan, Phys. Rev. E **62**, 3708 (2000).
[14] W. Chen and D.G. Gray, Langmuir **18**, 633 (2002).
[15] The function $\beta\Psi_{\mathrm{ex}}^{\mathrm{ref}}(\overline{\rho})$ in Eqs. (1) and (2) equals $\xi(4-3\xi)/(1-\xi)^2$, where $\xi=\pi\sigma_{eq}^3\overline{\rho}/6$ and $\sigma_{eq}^3=\sigma_{\perp}^2\sigma_{\parallel}$. The reference averaged density $\overline{\rho}_{\mathrm{ref}}$ is given by $(4\pi\sigma_{eq}^3/3)\overline{\rho_0}$, where $\overline{\rho_0}$ is the lowest-order component of the full weighted density $\overline{\rho}$.
[16] M.M. Telo da Gama, Mol. Phys. **52**, 585 (1984).
[17] T. J. Sluckin and A. Poniewierski, in *Fluid Interfacial Phenomena*, edited by C.A. Croxton (Wiley, New York, 1986), p. 215.
[18] A.K. Sen and D.E. Sullivan, Phys. Rev. A **35**, 1391 (1987).
[19] E. Velasco and L. Mederos, J. Chem. Phys. **109**, 2361 (1998).
[20] E. Martin del Rio, M.M. Telo da Gama, E. de Miguel, and L.F. Rull, Phys. Rev. E **52**, 5028 (1995).
[21] F.N. Braun, T.J. Sluckin, E. Velasco, and L. Mederos, Phys. Rev. E **53**, 706 (1996).
[22] Z.Y. Chen and J. Noolandi, Phys. Rev. A **45**, 2389 (1992).
[23] Z.Y. Chen, Phys. Rev. E **47**, 3765 (1993).
[24] P. Bolhuis and D. Frenkel, J. Chem. Phys. **106**, 666 (1997).
[25] F.N. Braun, T.J. Sluckin, and E. Velasco, J. Phys.: Condens. Matter **8**, 2471 (1996).